MOLECULAR AND CELLULAR BIOLOGY, Aug. 2005, p. 6427–6435 Vol. 25, No. 15
0270-7306/05/$08.00+0 doi:10.1128/MCB.25.15.6427–6435.2005

Polyadenylation and Degradation of Human Mitochondrial RNA: the Prokaryotic Past Leaves Its Mark†

Shimyn Slomovic,[1] David Laufer,[2] Dan Geiger,[2] and Gadi Schuster[1]*

Departments of Biology[1] and Computer Science,[2] Technion—Israel Institute of Technology, Haifa 32000, Israel

Received 23 March 2005/Returned for modification 18 April 2005/Accepted 12 May 2005

RNA polyadenylation serves a purpose in bacteria and organelles opposite from the role it plays in nuclear systems. The majority of nucleus-encoded transcripts are characterized by stable poly(A) tails at their mature 3′ ends, which are essential for stabilization and translation initiation. In contrast, in bacteria, chloroplasts, and plant mitochondria, polyadenylation is a transient feature which promotes RNA degradation. Surprisingly, in spite of their prokaryotic origin, human mitochondrial transcripts possess stable 3′-end poly(A) tails, akin to nucleus-encoded mRNAs. Here we asked whether human mitochondria retain truncated and transiently polyadenylated transcripts in addition to stable 3′-end poly(A) tails, which would be consistent with the preservation of the largely ubiquitous polyadenylation-dependent RNA degradation mechanisms of bacteria and organelles. To this end, using both molecular and bioinformatic methods, we sought and revealed numerous examples of such molecules, dispersed throughout the mitochondrial genome. The broad distribution but low abundance of these polyadenylated truncated transcripts strongly suggests that polyadenylation-dependent RNA degradation occurs in human mitochondria. The coexistence of this system with stable 3′-end polyadenylation, despite their seemingly opposite effects, is so far unprecedented in bacteria and other organelles.

Polyadenylation of RNA is a phenomenon common to all organisms examined to date. In eukaryotes, nucleus-encoded mRNA molecules are posttranscriptionally polyadenylated, a process important for their translation and longevity (6, 36). In contrast, in bacteria and organelles, excluding mammalian and trypanosomal mitochondria, RNA molecules are not stably polyadenylated (2, 3, 5, 6, 10, 14, 15). Instead, polyadenylation plays a central role in RNA degradation, which is thought to initiate by endoribonucleolytic cleavage of full-length RNA molecules. This step is believed to be carried out mainly by the endoribonuclease RNase E, in organisms which possess it (5, 16). The second stage of RNA degradation begins with the addition of poly(A) tails to the proximal end of the cleavage product, referred to as transient or internal polyadenylation, which targets the molecule for rapid 3′-to-5′ exonucleolytic degradation. The polyadenylation step is carried out by poly(A) polymerase (PAP) or polynucleotide phosphorylase (PNPase) (2, 5, 6, 22). Recently, a PAP was identified in human mitochondria (24, 34). The PNPase gene exists in the mammalian genome as well, and its product is targeted to mitochondria (26).

The human mitochondrial genome consists of a circular, double-stranded chromosome of about 16 kb which encodes 13 proteins, two rRNAs, and 22 tRNAs. Both strands of the mitochondrial DNA are transcribed, yielding polycistronic RNA precursors which are subsequently processed and stably polyadenylated to produce mature transcripts, which accumulate to different levels depending on their relative stabilities (8, 25, 32). Such a system requires an efficient and accurate RNA degradation mechanism which can differentiate between relatively stable molecules (rRNA and tRNA) and other transcripts, which must undergo rapid degradation (the intergenic region of the light [L] strand, for example). Although DNA replication, transcription, and RNA processing have been extensively studied during the last few decades, only limited progress has been made in the understanding of RNA degradation in mammalian mitochondria, and the molecular mechanism is as yet unknown.

As described above, mammalian mitochondrial transcripts differ from other prokaryotic systems by the presence of stable 3′ poly(A) tails, although their precise function is not entirely clear (8, 10, 32). However, one known function is the completion of partially encoded stop codons. During evolution, in several locations, condensation of the mammalian mitochondrial genome resulted in the appearance of incomplete stop codons, comprised of U or UA instead of UAA. At these locations, the posttranscriptional addition of poly(A) tails produces a functional translation stop codon.

Taking into account that in prokaryotes and organelles polyadenylation is part of RNA degradation, we asked whether mammalian mitochondria might feature destabilizing internal polyadenylation, in addition to stable 3′ polyadenylation. An alternative hypothesis suggested that human mitochondrial RNA (mtRNA), similar to the case in yeast mitochondria (7, 10; our unpublished results), is degraded without the participation of polyadenylation. We report here that human mtRNA molecules, of both cancer cell lines and primary fibroblasts, can be internally polyadenylated. Based upon the strict correlation between the presence of truncated, polyadenylated RNA molecules and the RNA degradation mechanism described above, in all of the systems in which it has been investigated, this internal polyadenylation is most likely part of the RNA deg-

* Corresponding author. Mailing address: Department of Biology, Technion, Haifa 32000, Israel. Phone: 972-4-8293171. Fax: 972-4-8295587. E-mail: gadis@tx.technion.ac.il.

† Supplemental material for this article may be found at http://mcb.asm.org/.

radation process. Therefore, despite the presence of stable poly(A) tails at the 3′ ends of their full-length transcripts, mammalian mitochondria indeed "remain true" to their prokaryotic origin and degrade RNA via the prokaryotic polyadenylation-dependent pathway.

MATERIALS AND METHODS

Cells. The cancer cell lines used in this work were CCRF-CEM T-cell leukemia, MCF-7 epidermal breast cancer cells, and CCRF-MTA (13). Primary human dermal fibroblasts were isolated from adult skin and cultivated as described previously (31).

RNA purification, RNA gel blots, and RT-PCR. RNA isolation was performed using the Invisorb Spin Cell-RNA Mini kit (Invitek Inc.). RNA gel blot analysis was performed as described previously (19). The hybridization probe for *COXI* was a DNA fragment spanning nucleotides (nt) 6150 to 6446 of the mitochondrial genome, which was ^{32}P labeled by random priming. The primers used for the amplification of this fragment from genomic DNA are listed in Table S8 in the supplemental material. A riboprobe was created for *ND6*, by T7 in vitro transcription of a DNA fragment covering nucleotides 14052 to 14374 of the L strand, using the primers outlined in Table S8 in the supplemental material. Oligo(dT)-primed reverse transcription-PCR (RT-PCR) was performed as described previously (18). Briefly, an adaptor $(dT)_{17}$ oligonucleotide was used to prime the RT reaction and the resulting cDNA was PCR amplified using the adaptor and one of the gene-specific primers shown in Table S7 in the supplemental material. PCR products were cloned and sequenced.

RNase H treatment. Oligonucleotide-directed cleavage using RNase H was used in order to remove the region containing the stable poly(A) tail located at the 3′ end of *COXI*. RNA (10 μg) and the oligonucleotide 5′-GAATGTGTG (0.3 μg) were denatured at 68°C for 10 min, annealed during slow cooling to 45°C, and incubated for cleavage at this temperature for 60 min with 2.5 units of RNase H.

RNase protection analysis. RNase protection experiments were performed as previously described (19). The antisense probes for analyzing the *COXI* and *ND6* 3′ ends were derived by T7 in vitro transcription of PCR-amplified templates. The primers used are listed in Table S2 of the supplemental material. The ^{32}P-uniformly labeled antisense RNA probes were designed to include 10 to 15 nonrelated nucleotides at their 5′ ends in order to allow differentiation between any remaining nondigested probe and fully protected probe. Subsequent to DNase treatment, total RNA was annealed to the probe at 50°C overnight. Digestion was performed with 120 units of RNase T_1 for 60 min. The RNA was then purified and fractionated through 5% polyacrylamide-7 M urea sequencing gels along with RNA markers. For the analysis of *COXI* and *ND6*, 20 μg and 30 μg of total RNA were used, respectively.

The PolyAfinder tool. The PolyAfinder tool (http://bioinfo.cs.technion.ac.il/sdata/PolyAFinder/HTML/polyAFinder.html) was established in order to search the human expressed sequence tag (EST) database for ESTs originating from polyadenylated mitochondrial transcripts. The PolyAfinder program accepts a variety of parameter settings, such as subsequence length, added poly(A) length, jump size between subsequences, and BLAST match percentage. For our work, we used the tool in the following manner. A sequence of eight adenosines was added 3′ to a 25-nt-long subsequence, derived from a designated location in the human mitochondrial genome. A homology search based on the human EST database at 100% homology, using the BLAST algorithm, was then applied to this 33-nt sequence. At this stage, the resulting positive ESTs were collected. The 25-nt subsequence frame was shifted 1 nt downstream, and the process was repeated, creating a cycle which continued until the end of the genomic sequence was reached. The accumulated results were then filtered according to several strict criteria in order to ensure that only authentic ESTs, representing mitochondrial transcripts with posttranscriptionally added poly(A) tails, were included in the final results. Further software details are listed at the website above.

RESULTS

Detection of nonabundant, internally polyadenylated *COXI* transcripts by reverse transcription-PCR. Our initial goal was to examine the possibility that the prokaryotic poly(A)-dependent degradation pathway operates in human mitochondria. We hypothesized that, if this is indeed the case, truncated, internally polyadenylated RNA molecules would be present. The mtRNA encoding subunit I of cytochrome oxidase (*COXI*) was chosen as a representative mitochondrial transcript. Following transcription of the polycistronic RNA extending along the entire heavy (H) strand of the mitochondrial genome, the *COXI* mRNA is produced by processing and the addition of a stable poly(A) tail at its 3′ end (25). Two methods were applied for the detection of the hypothesized nonabundant internally polyadenylated transcripts. In the first, oligo(dT)-primed RT followed by PCR amplification with specific primers was used. This method has successfully detected such molecules in prokaryotes and organelles (18, 28). The second method entailed bioinformatically screening the human EST databases, whose cDNAs were primarily generated by priming with oligo(dT).

During the first approach, RNA of either human cancer cell lines or primary fibroblasts was purified and analyzed. Initially, the isolation of nonabundant, internally polyadenylated *COXI* molecules was hampered by the abundance of full-length *COXI* transcripts containing stable poly(A) tails located at the end of the $tRNA^{Ser(UCN)}$ antisense sequence, which immediately follows the *COXI* open reading frame (ORF) (Fig. 1A). Fifty-one such clones were isolated, along with an additional 11 clones containing poly(A) tails exactly at the end of the *COXI* ORF (Fig. 1A). In order to eliminate this dominant population of polyadenylated molecules, we added an initial step of oligonucleotide-directed RNase H cleavage to remove the 3′-end region of *COXI* containing the stable poly(A) tails. Following this cleavage, oligo(dT)-primed RT was performed and the resulting cDNA molecules were amplified with *COXI*-specific primers. Amplification products were then cloned and analyzed by DNA sequencing.

As shown in Fig. 1A and Table S1 (in the supplemental material), numerous *COXI* transcripts with internal polyadenylation sites were identified. Although a number of polyadenylation positions were clustered (following the second primer in Fig. 1A), we cannot exclude the possibility that this result reflects the higher efficiency of this primer rather than a hotspot for cleavage and/or polyadenylation. Indeed, the fact that the bioinformatic analysis discussed below did not show this clustering (Fig. 1B) is in agreement with the "efficient primer" alternative. The poly(A) tails were homogeneous, and their lengths ranged between several and 72 adenosines (Table S1 in the supplemental material). However, the exact length of the original poly(A) tract cannot be determined using this method, as the oligo(dT) primer used to synthesize the first-strand cDNA during the RT procedure can anneal to the poly(A) tail at any point. The requirement for 30 PCR cycles to detect the internally polyadenylated transcripts implied that these molecules are present at a low level relative to that of full-length transcripts with stable poly(A) tails.

Detection of ESTs corresponding to internally polyadenylated *COXI* transcripts using a bioinformatic tool. The human EST database includes approximately 6 million entries, mostly resulting from oligo(dT) priming. We assumed that, if fragmented polyadenylated mitochondrial transcripts indeed existed, their corresponding ESTs would be among these accessions. In order to detect these specific ESTs, the "PolyAfinder" tool was developed and used in the following manner: eight adenosines were added to the 3′ end of the first 25 nt, in this case of *COXI*. A BLAST search of the human EST database

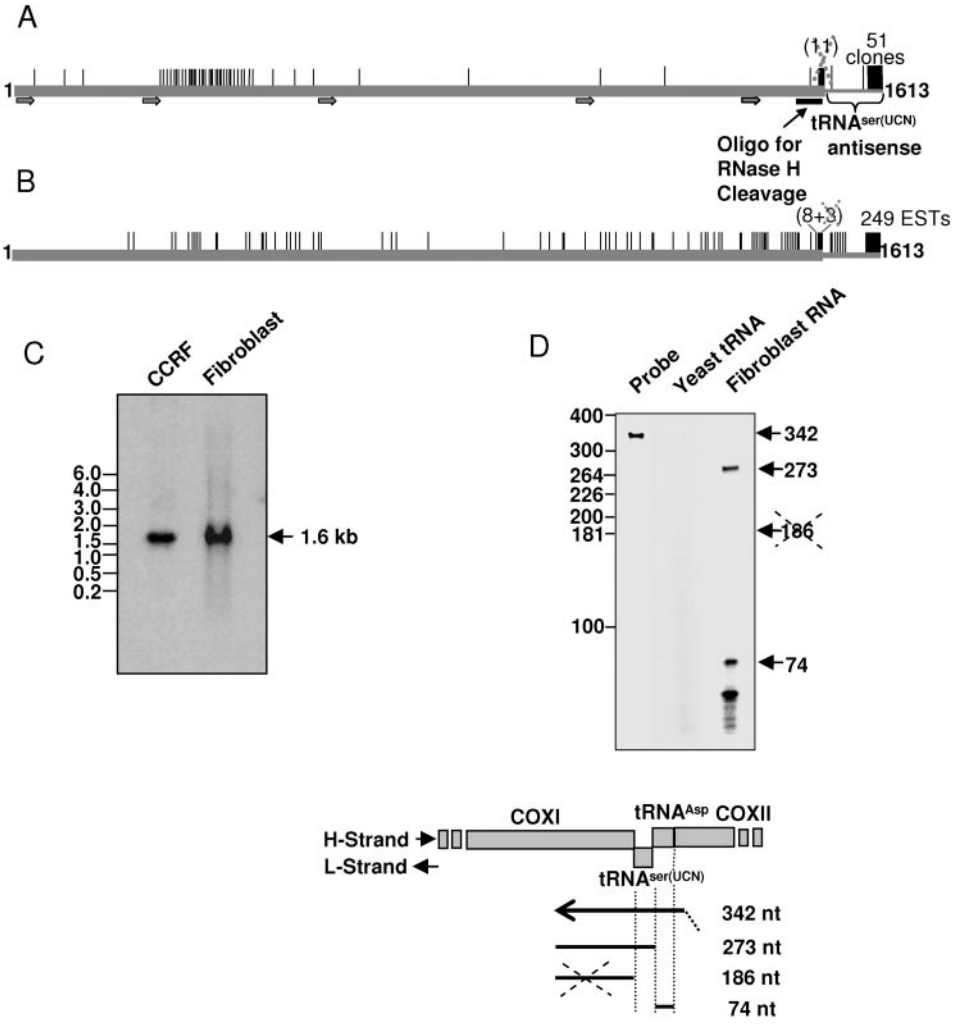

FIG. 1. Analysis of truncated and polyadenylated *COXI* transcripts. A. Analysis using RT-PCR. The *COXI* transcript is schematically presented including the antisense region of $tRNA^{Ser(UCN)}$ (thin gray line). The primers used for PCR amplification of the oligo(dT)-primed cDNAs are shown by arrows below. The location of the oligonucleotide used for the RNase H-directed cleavage to remove the region containing the stable poly(A) tail is indicated by a horizontal black bar. Thin vertical lines indicate the positions of poly(A) tail addition. The dashed vertical line at the end of the *COXI* ORF designates an abundant but false polyadenylation position resulting from a gene-encoded poly(A) tract. Indeed, the poly(A) tails of these clones were shorter than 17 nt (see the supplemental material). Details concerning the polyadenylation positions and tail lengths are in the supplemental material. B. Analysis using PolyAfinder. *COXI* polyadenylation sites found in ESTs are presented as described for panel A. Of the 11 ESTs found at the end of the ORF, eight contained poly(A) tails longer than 17 adenosines. These were therefore considered authentic rather than resulting from annealing of the oligo(dT) primer to the A_6 tract located nearby. C. RNA gel blot analysis of *COXI*. Total RNA was isolated from the cancer cell line CCRF-CEM and primary fibroblasts, and a gel blot was probed with a ^{32}P-labeled double-stranded *COXI* probe. The migration of molecular size markers (in kilobases) is shown at the left. D. RNase protection assay to define the *COXI* mRNA 3′ end. Total RNA isolated from primary fibroblasts was annealed to a uniformly labeled probe of 342 nt spanning *COXI*, the antisense region of $tRNA^{Ser(UCN)}$, $tRNA^{Asp}$, and several bases of *COXII* and ending with nine unrelated nucleotides. A parallel control reaction substituted an equivalent amount of yeast tRNA. The reaction mixtures were treated with RNase T_1, and the protected fragments were analyzed by gel electrophoresis and autoradiography. The positions of RNA molecular size markers in nucleotides are shown at the left. The locations and sizes of the undigested probe and protected fragments are indicated to the right in the diagram below.

was applied to this 33-nt sequence, and EST matches with 100% identity were collected. The 25-nt subsequence frame was shifted 1 nt downstream, and the process was repeated, creating a cycle which continued until the end of the *COXI* sequence. The accumulated ESTs were then filtered according to several criteria which verified their authenticity.

In the final analysis, 249 ESTs were found containing the stably polyadenylated 3′ end of the antisense $tRNA^{Ser(UCN)}$ region, and 80 corresponding to fragmented, polyadenylated *COXI* transcripts, in 69 sites dispersed throughout the gene (Fig. 1B). It should be noted that this number is a minimal estimate, as many additional ESTs related to fragmented polyadenylated *COXI* transcripts were excluded due to mismatches resulting most probably from sequencing errors. These ESTs were obtained upon reducing the stringency of the search to less than 100% identity (data not shown). Other ESTs showed high homology when aligned with certain nuclear chromosomal sequences which are highly (>90%) identical to mito-

chondrial DNA (37). It is assumed that these pseudogenes are not transcribed, and therefore we concluded that all positive ESTs were derived from internally polyadenylated mitochondrial transcripts. Together with the RT-PCR results derived from both primary fibroblasts and cancer cell lines, this in silico observation of numerous fragmented, polyadenylated *COXI* transcripts strongly suggested that the bacterial and organellar poly(A)-dependent RNA degradation mechanism operates in human mitochondria.

Antisense tRNA$^{Ser(UCN)}$ forms the 3′ untranslated region of the *COXI* transcript. As stated above, oligo(dT)-primed RT-PCR performed without initially removing stable poly(A) tails yielded a majority of clones with poly(A) tails at the end of the tRNA$^{Ser(UCN)}$ antisense sequence. However, 11 clones representing polyadenylation at the translation stop codon of *COXI* were obtained, and several corresponding ESTs were revealed using PolyAfinder. Upon further investigation, a tract of six encoded consecutive adenosines, positioned immediately downstream of the *COXI* stop codon, was noted. We considered the possibility that these adenosines might anneal to oligo(dT) prior to RT-PCR and therefore be the cause of both the clones and the ESTs which appeared to contain a poly(A) tail at this position. Since the 3′ end of *COXI* was mapped previously to the end of the antisense sequence of tRNA$^{Ser(UCN)}$ (25), we asked whether, in addition, the *COXI* transcript exists in a form which terminates at the translation termination codon.

RNA gel blot analysis revealed a single major *COXI* transcript of 1.6 kb in both cell types; however, this type of analysis did not provide adequate resolution to determine if both forms of *COXI* existed (Fig. 1C). The observation of a single high-molecular-weight hybridization signal further supported our hypothesis that the truncated polyadenylated transcripts are heterodisperse, do not accumulate, and are rapidly degraded (Fig. 1C and 2B). In order to characterize more accurately the *COXI* mRNA 3′ end, RNase protection analysis was performed. An antisense ^{32}P-RNA probe, spanning the *COXI* 3′ end, tRNA$^{Ser(UCN)}$ antisense, tRNA^{Asp}, and ending with several unrelated nucleotides, was annealed to total RNA and digested with RNase T_1 (Fig. 1D). The product sizes were determined following denaturing polyacrylamide gel electrophoresis, and no fragment of 186 nt, which would result from a major *COXI* transcript ending at the translation termination codon, was detected. The major product was 273 nt and represented *COXI* mRNA terminating at the 3′ end of the antisense strand of tRNA$^{Ser(UCN)}$. Additionally, the 74-nt product representing tRNA^{Asp} was detected. It should be noted that, since RNase T_1 was used, which cleaves at guanosine residues in single-stranded RNA, the exact lengths of protected fragments were related to the first guanosine of the probe, found beyond the 3′ end of the probe-protecting *COXI* RNA fragment. The lack of any protected bands in the control lane, in which total RNA of human cells was replaced by yeast tRNA, shows the specificity and accuracy of this analysis. The protected short RNA molecule that appears below the band of tRNA^{Asp} is most likely due to incomplete unfolding or refolding of the tRNA during the assay, as reported previously (35). These results revealed that mature *COXI* mRNA exists in a single form with its 3′ end including the full antisense sequence of tRNA$^{Ser(UCN)}$.

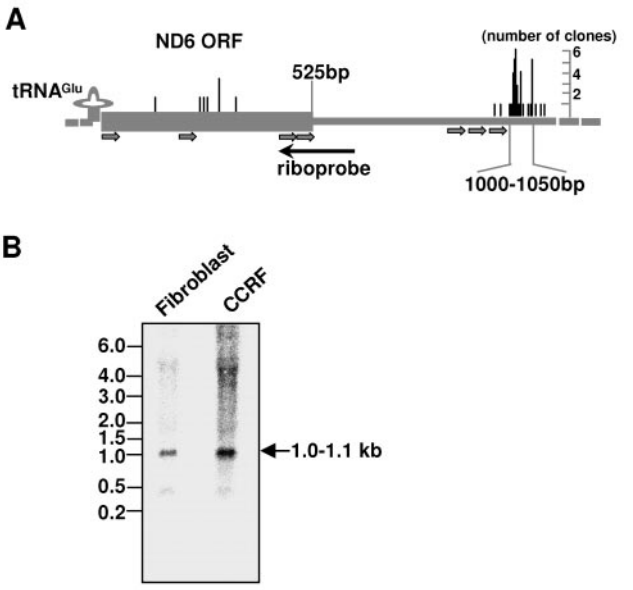

FIG. 2. Polyadenylation of *ND6* transcripts. A. Polyadenylation analysis using RT-PCR. The *ND6* transcript from the first AUG to the translational termination codon is presented as a thick gray line ending at position 525. The downstream region is presented as a thin gray line, and tRNA^{Glu}, located upstream of *ND6*, is indicated by a cloverleaf structure. Below the diagram, PCR primers are shown as gray arrows, and the antisense riboprobe is shown as a horizontal arrow. Thin vertical lines indicate the positions of poly(A) addition, with lengths proportional to the number of clones obtained. B. RNA gel blot analysis of *ND6*. Analysis was carried out as described in the legend to Fig. 1C, except that the probe was the uniformly labeled antisense RNA shown in panel A.

Detection of nonabundant, internally polyadenylated *ND6* transcripts. *ND6* is the sole protein-encoding gene located on the L strand. Therefore, it was chosen as the second mRNA for polyadenylation analysis. Its mRNA accumulates at a much lower level than that of *COXI*, and its polyadenylation status was not reported, as its exact 3′ end was not defined (11, 23, 25). We used several primers positioned along the ORF for oligo(dT)-primed RT-PCR analysis, as described for *COXI*. Indeed, as expected of a nonabundant transcript, more amplification and screening steps were required than for *COXI*. However, we were successful in isolating several fragmented *ND6* transcripts with polyadenylation sites distributed along the ORF, using RNA from either cancer or fibroblast cells (Fig. 2A; Table S2 in the supplemental material). As for *COXI*, the *ND6* poly(A) tails were homogeneous. Analysis of the *ND6* ORF, using PolyAfinder, yielded only one positive EST, most likely due to the low accumulation of this transcript (see the supplemental material).

Defining the 3′ end of the *ND6* mRNA. Similar to the H strand, the L strand is fully transcribed, followed by processing mostly at the tRNA punctuation points (25). However, no tRNA gene is located in close proximity to the stop codon of *ND6*, and accordingly, an mRNA much longer than the 525-nt ORF has been reported (11, 35). Since no stably polyadenylated transcripts were identified at the exact end of the ORF using RT-PCR or PolyAfinder, we decided to determine the *ND6* 3′ end. RNA gel blot analysis using a riboprobe which

covered the 3′ end of the ORF and the adjacent downstream region revealed, as previously reported, one major band of 1.0 to 1.1 kb (Fig. 2B) (1, 11, 35), whether RNA was extracted from cancer cells or from primary fibroblasts. In spite of high-stringency conditions, longer and heterodisperse transcripts were also detected and likely originate from unprocessed or partially processed L-strand pre-RNAs (Fig. 2B).

As the *ND6* ORF is 525 nt and the 5′ end is located at the adenosine of the first AUG, the RNA gel blot analysis result was consistent with a 500- to 600-nt-long 3′ untranslated region, a rarity in human mtRNA. Accordingly, three additional primers were used for RT-PCR-based polyadenylation analysis of the region 900 to 1,100 nt downstream of the start codon. In this experiment, we were able to isolate many cDNAs corresponding to transcripts harboring poly(A) tails of up to 51 adenosines, mainly mapping 1,000 to 1,050 nt downstream of the AUG (Fig. 2A; Table S2 in the supplemental material). As stated earlier, the exact length of the poly(A) tails could not be determined due to the possibility of dT-primer annealing at any given point. The polyadenylation sites in these transcripts spanned a small region of ~50 nt. Together with the RNA gel blot analysis, these results suggested that the 3′ end of *ND6* mRNA is located in this area. However, these results also suggested that, in contrast to the *COXI* 3′ end, which shows consistent polyadenylation at a single position, the full *ND6* transcript has multiple 3′ ends. Unlike *COXI*, for which RT-PCR results were supported by PolyAfinder, the tool was unsuccessful in locating *ND6* ESTs showing polyadenylation at this downstream region, even when stringency conditions were lowered. This could be explained by the much lower level of *ND6* transcripts than of those of *COXI*. In order to further study the 3′ ends of *ND6* mRNA, RNase protection analysis was performed.

A 333-nt probe extending beyond the 3′ end of the *ND6* ORF and terminating with 10 unrelated nucleotides was produced (Fig. 3A, probe I). Following RNase T_1 digestion and gel analysis (Fig. 3B), no product of 293 nt, corresponding to a transcript which terminates at the stop codon, was detected. This was in agreement with the RNA gel blot analysis. However, a product of 324 nt, matching the full-length probe (minus the digested unrelated sequence), was shown to be protected, demonstrating that the *ND6* transcript indeed continues further downstream. Therefore, a second probe covering positions 900 to 1219 downstream of the first AUG was designed. This 334-nt probe included 15 unrelated nucleotides (Fig. 3A, probe II). Based on the RT analysis results which suggested ragged *ND6* 3′ ends, we suspected that a single, well-defined product would not be obtained. Instead, we anticipated products of various lengths, corresponding to the first guanosine residues beyond the 3′ ends of the transcript fragments which terminate in this area.

Several nonrelated negative-control RNA sources were first analyzed, and experimental conditions were defined in which no protected bands accumulated. These RNA preparations included yeast tRNA, total chloroplast RNA from *Arabidopsis thaliana*, *Escherichia coli* RNA, and RNA isolated from the halophilic archaeon *Haloferax volcanii*. This step was critical for the success of this experiment, as the relatively low abundance of *ND6* transcripts made it necessary to increase the amount of input RNA. When total RNA from several cell lines was analyzed under these optimized conditions, the expected products, of lengths ranging up to 164 nt, were detected from human RNA preparations but not controls (Fig. 3C). In addition to these products, a 321-nt fragment representing the full-length probe minus unrelated sequences was detected, indicating that, despite the processing which produces the ~1,050-nt *ND6* transcript, the longer unprocessed transcript also accumulates significantly, as previously reported (Fig. 3C) (11, 25, 35). The lack of protected fragments between 321 and 164 nt also supports the conclusion that the detected products represent genuine *ND6* 3′ ends, which terminate 1,000 to 1,050 nt downstream of the first AUG, and that 3′ maturation occurs

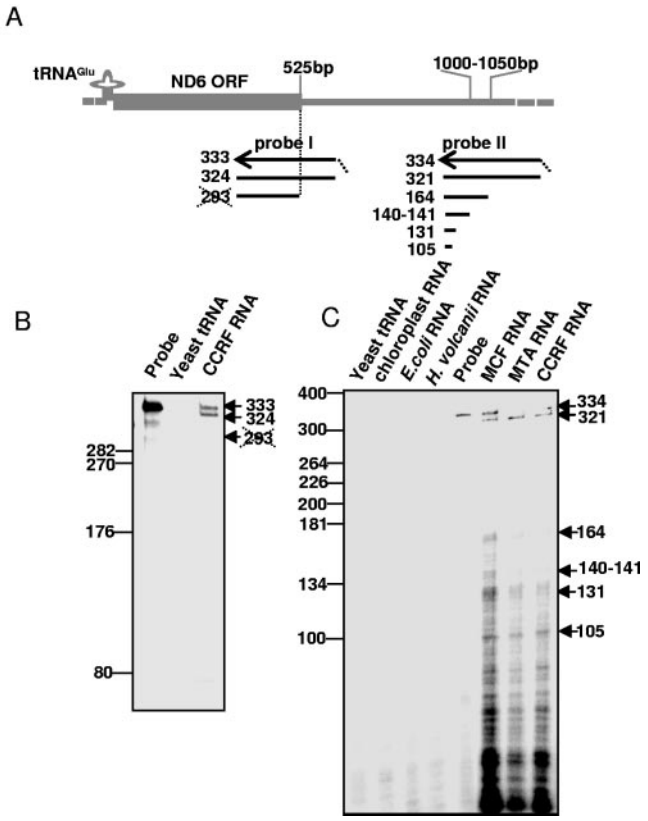

FIG. 3. The heterogeneous 3′ termini of *ND6* mRNA are located ~500 nucleotides downstream of the translation termination codon. A. The *ND6* region is schematically presented as described for Fig. 2A. Probe I (333 nt) is complementary to a segment of the ORF and the immediate downstream region and ends with 10 unrelated nucleotides. An *ND6* transcript terminating at the stop codon would be expected to protect a 293-nt fragment; this product was not observed, and therefore the line representing it is crossed out. Probe II (334 nt) covers the downstream region in which poly(A) addition sites were located by RT-PCR. The full-length probe and the predicted protected products are presented. B. RNase protection analysis using probe I. Total RNA isolated from CCRF-CEM cancer cells was annealed with probe I and analyzed as described in the legend to Fig. 1D. The position where product of 293 nt would migrate is shown, and the positions of the observed 324-nt product and the full-length probe are indicated at the right. C. RNase protection analysis using probe II. Total RNA was isolated from three cancer cell lines (CCRF-CEM, CCRF-CEM/MTA, and MCF-7) as well as four negative controls including equal amounts of yeast tRNA, *Arabidopsis thaliana* chloroplasts, *E. coli*, and *Haloferax volcanii* RNAs. The migration of RNA markers is indicated at the left, and the probe and protected bands are shown at the right.

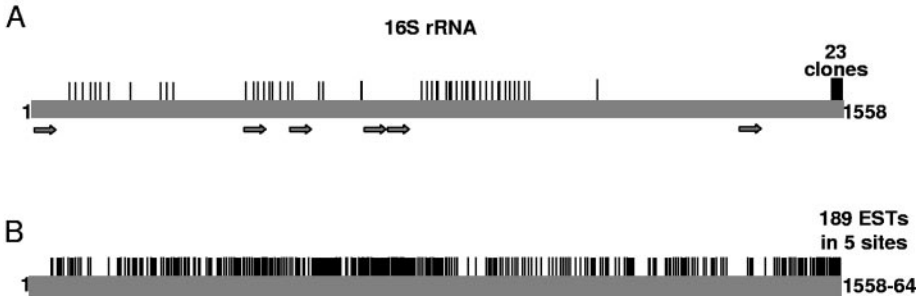

FIG. 4. Polyadenylation of 16S rRNA. A. Analysis using RT-PCR. The transcript is presented schematically with the locations of PCR primers indicated by gray arrows. Thin vertical lines indicate the positions of poly(A) addition. B. Analysis using PolyAfinder. Sites of polyadenylation found in ESTs by PolyAfinder are presented as for panel A.

in this short region. Together, the combined results of the RT-PCR-generated 3′ polyadenylated *ND6* transcripts, the RNA gel blot assay, and the RNase protection analysis strongly suggest that the 3′ end of *ND6* mRNA is located 500 to 550 nt downstream of the translation termination codon and, unlike the precise 3′ ends of H-strand transcripts, spans an area of about 50 nt.

Detection of internally polyadenylated 16S rRNA. After demonstrating the presence of truncated, polyadenylated transcripts of protein-coding genes from both the H and L strands, we asked if mitochondrial rRNA undergoes this process as well, as it does in bacteria and organelles (2, 20, 28). The rRNAs were previously reported to possess stable poly(A) tails at their 3′ ends (25). The 16S rRNA gene, which is encoded on the H strand, was chosen for this analysis. Polyadenylation analysis results for this gene were obtained with fewer PCR cycles and selection steps than in the cases of *COXI* and especially *ND6*, due to the high abundance of the rRNA. Accordingly, the removal of the stable 3′-end poly(A) tail by RNase H-directed cleavage was unnecessary. We obtained cDNAs corresponding to numerous fragmented transcripts, polyadenylated at sites throughout much of the 16S rRNA, using RT-PCR (Fig. 4A). Using PolyAfinder, more than 740 related ESTs were detected (Fig. 4B; Tables S3 and S6 in the supplemental material). Although sites were dispersed along the molecule, the frequency of polyadenylation at each internal site was much lower than that of the polyadenylation site located at the mature 3′ end. As in the case of *COXI*, this observation, along with the wide dispersion of internal sites, suggests that the truncated molecules are integral to the RNA degradation process.

Internal polyadenylation of tRNA. Since truncated, polyadenylated mRNAs and rRNAs are present in mitochondria, we decided to determine if truncated polyadenylated tRNAs could be found as well. Following transcription, the 5′ and 3′ ends of the tRNA are formed by endonucleolytic cleavage of the precursor polycistronic RNA by RNase P and RNase Z, respectively. Subsequent to RNase Z cleavage, a CCA tail is added to the 3′ end and several nucleotides are modified to create a functional molecule (17).

Similar to *ND6*, tRNAs are not known to possess stable 3′-end poly(A) tails. As a representative of H-strand-encoded tRNAs, $tRNA^{Lys}$, located between *COXII* and *ATP8-ATP6-COXIII*, was analyzed. In this tRNA, several nucleotides undergo posttranscriptional modifications that were shown to be essential for correct folding and activity (12). RT-PCR identified 20 cDNAs corresponding to truncated $tRNA^{Lys}$; these transcripts possessed poly(A) tails of up to 52 nt in length. One additional cDNA was revealed using PolyAfinder (Fig. 5A; Table S4 in the supplemental material). However, no $tRNA^{Lys}$ cDNAs were obtained in which a poly(A) tail had been added to the mature 3′ end, either before or after addition of the CCA tail. This result suggested that the 3′ end of $tRNA^{Lys}$ is not available for polyadenylation by PAP and/or PNPase.

Previously, it was argued that, following transcription, part of the tRNA population is immediately digested, with only some undergoing base modification and CCA addition (12). Our analysis was unable to clarify whether the nonmodified population, the mature and active one, or both undergo polyadenylation. The $tRNA^{Gln}$ was analyzed as a representative of L-strand tRNAs, and cDNAs corresponding to a number of internally polyadenylated molecules were isolated (Table S5 in the supplemental material). Together, these results suggest that tRNA degradation in human mitochondria is performed by the polyadenylation-dependent degradation pathway.

Polyadenylation of D-loop transcripts. The D-loop region is noncoding and contains the main regulatory elements for transcription and DNA replication. Analysis of this region for ESTs representing polyadenylated RNAs revealed a relatively high number of ESTs derived from both H- and L-strand transcripts (Fig. 5B; Table S6 in the supplemental material). In the case of the L strand, most of the ESTs were located in the vicinity of the origin of the H-strand DNA replication point, where the triple-stranded structure of the D loop begins (8, 9, 25, 29). These ESTs are probably derived from transcription initiation at the L-strand promoter and represent cleaved molecules that serve as primers for H-strand replication. Indeed, such polyadenylated RNAs, numbered 18 by the Attardi group, were previously detected (25). As for the ESTs related to polyadenylated RNAs of the H strand in this region, the poly(A) addition sites of 14 ESTs were located immediately upstream of the H-strand transcription initiation site (Fig. 5B; Table S6 in the supplemental material). These ESTs could be derived from the full-length H-strand transcript, which terminates at this location.

Polyadenylation of the entire mitochondrial transcriptome. After successfully finding evidence for truncated, polyadenylated RNA molecules for each mitochondrial gene examined, we decided to use PolyAfinder to analyze the entire human

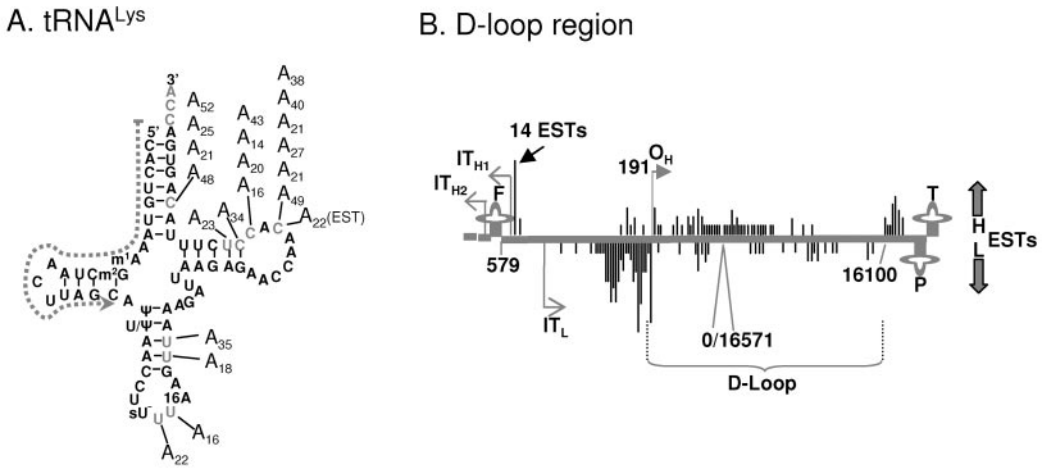

FIG. 5. A. Polyadenylation of $tRNA^{Lys}$. The positions of poly(A) addition and tail lengths as determined by RT-PCR are shown in gray. In cases in which polyadenylation occurred in close proximity to a DNA-encoded adenosine, the stated tail length includes this residue. The PCR primer is represented as a dashed gray arrow. B. Polyadenylation analysis of the D-loop region. The region between $tRNA^{Thr}$ and $tRNA^{Phe}$, which includes the D loop, is presented schematically. The positions of poly(A) addition revealed by the PolyAfinder are indicated by vertical lines above or below for the H and L strands, respectively. The length of each line is proportional to the number of ESTs found at that location. The transcription initiation sites on the H (IT_{H1} and IT_{H2}) and L (IT_L) strands as well as the origin of replication on the H strand (O_H) are indicated. The tRNAs are represented by cloverleaf symbols using single-letter designations for the amino acids.

mitochondrial transcriptome. The results are presented schematically in Fig. 6, and details are in Table S6 in the supplemental material. A total of 2,545 and 186 ESTs terminating at 818 and 94 sites were identified for the H and L strands, respectively. These included ESTs corresponding to truncated, polyadenylated transcripts of mRNAs, rRNAs, tRNAs, and L-strand intergenic regions. The number of ESTs found for each molecule was proportional to the accumulation level of that particular transcript. Therefore, the most abundant were the rRNA ESTs and the least abundant were those related to the L-strand intergenic regions, which undergo rapid degradation. The EST results showed expected polyadenylation "hotspots" representing stable polyadenylation at the mature 3′ ends of most of the mtRNAs, the most often recurring one being at the *COXI* 3′ end, where 249 ESTs were found (Fig. 6). Exceptions are *ND6*, described above in this work, and *ND5*. Of the 94 L-strand sites, 52 were located within or near the D loop and are discussed above.

DISCUSSION

Using both experimental and bioinformatic approaches, we demonstrated that human mtRNA of both the H and L strands is internally polyadenylated, strongly suggesting that a prokaryotic polyadenylation-dependent degradation mechanism exists in this system. The endonucleolytic cleavage thought to initiate this pathway is believed to be performed by the endoribonuclease RNase E in organisms in which it is present (2, 5, 16). However, no RNase E-encoding gene is found in the human genome, and the enzyme seems to be generally absent from mitochondria. If not RNase E, which endoribonuclease initiates RNA degradation in human mitochondria? Two endoribonucleases, RNase P and RNase Z, which perform the processing of the 5′ and 3′ ends of the tRNAs, respectively, have already been characterized in human mitochondria (17). At points of tRNA punctuation, characteristic of the mitochondrial genome, RNase P cleavage produces the 3′ end of the nascent upstream mRNA which is subsequently stably polyadenylated. This enzyme could be responsible for the internal cleavages that initiate RNA degradation as well. Alternatively, RNase Z or an endoribonuclease yet to be identified could solely be responsible for, or at least contribute to, this process. Revealing the nature, specificity, and control mechanism of this enzyme will shed light on the initial step of the RNA degradation process. Indeed, it is the control of this step which is believed to be crucial for determining the half-life of the corresponding transcript (2, 16).

Following the endonucleolytic cleavage the proximal cleavage product is either degraded by exoribonucleases or polyadenylated by PAP or PNPase and then degraded (2, 5, 16, 27). In *E. coli*, the polyadenylation is performed mainly by PAP I, a nucleotidyltransferase homologue, and to a much lower extent by PNPase (21, 22). In spinach chloroplasts, cyanobacteria, and the bacterium *Streptomyces coelicolor*, this process is performed by PNPase alone, which unlike PAP creates heterogeneous tails, containing other nucleotides in addition to adenosines (2, 18, 28, 30, 38). Transcripts containing heterogeneous poly(A)-rich tails could have been successfully isolated using the dT-primed RT-PCR method used here, as the primer will anneal to regions of the tail particularly rich in adenosine. In such a case, the 3′ end of the resulting clone contains consecutive adenosines corresponding to the dT primer and a heterogeneous region progressing 5′ towards the cleavage site of the transcript.

Although PNPase is present in human mitochondria (26), the homogeneity of the poly(A) tails revealed here suggests that they are formed by a PAP. Indeed, PAP is also found in human mitochondria (24, 34). Inactivation of this enzyme resulted in a decrease in the lengths of the 3′ stable poly(A) tails, from about 50 adenosines to only eight, suggesting the pres-

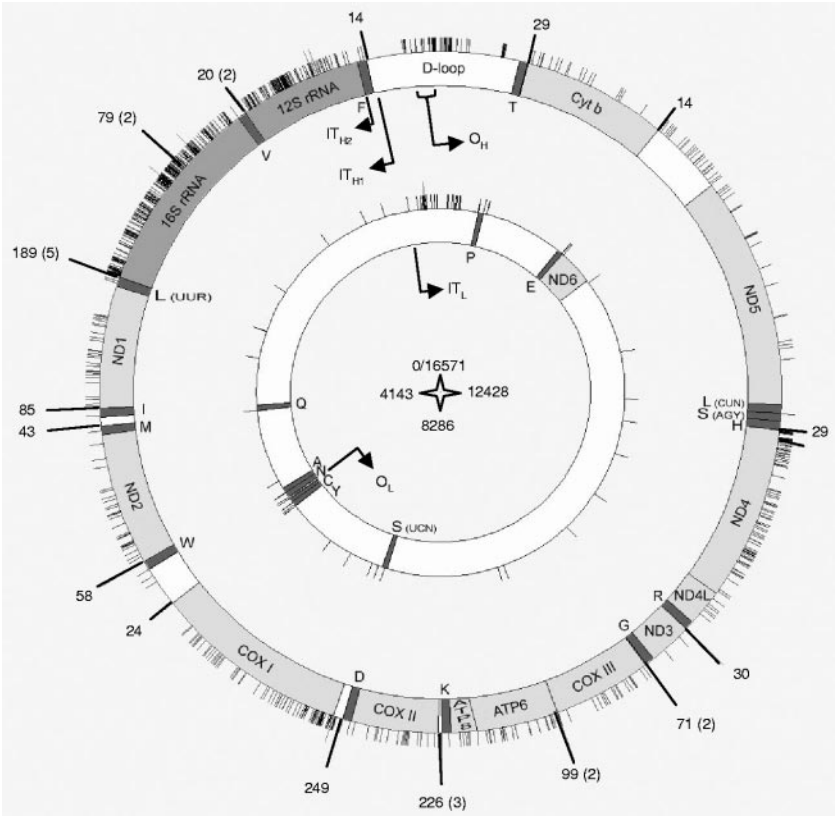

FIG. 6. Analysis of the human EST database for polyadenylated mitochondrial transcripts. Poly(A) addition positions revealed by PolyAfinder are indicated by radial lines. The external and internal circles represent the H and L strands, respectively. Long lines represent sites for which >10 ESTs were found, with the precise number indicated beside the line. When several such sites are clustered, the number of sites is indicated in parentheses. The tRNA genes are indicated by single-letter symbols. The origins of replication and transcription initiation sites are denoted as in Fig. 5B.

ence of additional or alternative polyadenylation activity (34). Hence, this PAP could be the enzyme responsible for the internal polyadenylation. However, the involvement of PNPase or another PAP cannot be excluded.

The third step of poly(A)-dependent RNA degradation is the exonucleolytic degradation of the polyadenylated cleavage product, which is performed by the exoribonucleases PNPase and a member(s) of the hydrolytic enzymes of the RNR family. In *E. coli*, the members of the RNR family are RNase II and RNase R, and are both involved in the degradation of polyadenylated RNAs (4). Human mitochondria harbor PNPase and therefore either alone or together with a member of the RNR family, yet to be identified, it could be involved in the poly(A)-dependent degradation pathway. As stated, a major and unique difference between this system and bacteria/organelles, in which this pathway has been analyzed, is the fact that, in human mitochondria, both stable and degradation-associated poly(A) tails coexist. What is the mechanism that allows differentiation between these two types of tails, which results in opposite outcomes concerning the stability of the transcript? Previously, it has been suggested that, similar to nucleus-encoded RNA, the stable 3′ poly(A) tail is protected by a poly(A)-binding protein (33). In such a scenario, the varying ability of such a protein to bind a mature 3′-end tail, as opposed to internal tails, could determine the nature of the tail, stable or unstable, and consequently that of the transcript. Such a poly(A)-binding protein has yet to be identified in human mitochondria. Translation and protection by ribosomes do not seem to be the answer, as rRNA itself is polyadenylated both internally and at the 3′ end. Concerning the poly(A) tails located at the 3′ end of the transcript, a correlation between tail length and RNA stability was observed (33). While transcripts with short poly(A) tails were degraded, those possessing longer tails were stable. Interestingly, opposing effects of polyadenylation on the stability of edited and unedited mtRNAs in *Trypanosoma brucei* were recently obtained (14).

The entire function of the stable 3′ poly(A) tails of most mitochondrial transcripts is still unknown. In several cases, the formation of this tail establishes the complete translation termination codon (25). It is possible that the poly(A) tails protect and prevent degradation of the 3′ end of the transcript. In agreement with previous studies, our bioinformatic analysis shows that all transcripts punctuated by tRNAs are stably polyadenylated, subsequent to RNase P cleavage at these precise sites (25) (Fig. 6). However, as shown in this work, *ND6*, for example, which is not punctuated by a downstream tRNA and therefore is processed differently, is not stably polyadenylated at a precise point. Processing of tRNA 3′ ends, including CCA addition, is probably a very efficient process which successfully competes with polyadenylation. Indeed, no cDNAs corresponding to polyadenylated mature tRNAs were detected, although internal polyadenylation was.

Our analysis of polyadenylated ESTs shows that every transcript originating from the human mitochondrial genome, including the intergenic regions of the polycistronic transcripts and RNA primers for the H-strand DNA replication, can be polyadenylated by stable and/or internal, unstable poly(A) tails. Therefore, internal polyadenylation is a common and characteristic aspect of mammalian mitochondrial transcripts, as is the case with other bacteria and organelles. An exception is yeast mitochondria, in which neither polyadenylation nor PNPase has been detected (7, 10).

When considering the possible evolutionary development of the polyadenylation phenomenon witnessed in bacteria, organelles, and nucleus-encoded transcripts, it is tempting to suggest a possible scenario in which, in mammalian mitochondria, stable 3′-end polyadenylation evolved from the transient polyadenylation acquired from the bacterial ancestor. Condensation of the mammalian mitochondrial genome during evolution resulted in incomplete translation termination codons, which made stable 3′ polyadenylation indispensable. Perhaps subsequently, stable poly(A) tails in the nucleus were added, and a function in translation initiation arose, through evolution. Indeed, the initial step in polyadenylation, endoribonucleolytic cleavage, is shared by bacteria, mammalian mitochondria, and the nuclear polyadenylation apparatus. Alternatively, the two types may have evolved separately and later coalesced in mammalian mitochondria.

ACKNOWLEDGMENTS

We thank Ilan Ifergan, Asaf Shafran, Yehuda G. Assraf, Ifat Sher, Simona Zisman, and Dina Ron for the cancer cells and primary fibroblasts; Shiri Solsky and Shachar Uliel for excellent technical assistance; and Victoria Portnoy for the archaeal RNA. We thank members of our laboratory and Robert Lightowlers for critical reading of the manuscript and Jan Piwowarski for the idea of searching the human EST database. Special thanks go to David Stern for critically reading and editing the manuscript.

This work was supported by grants from the Israel Science Foundation (ISF) to G.S. and D.G. and from the Binational Science Foundation (BSF) and Binational Agriculture Science and Development Foundation (BARD) to G.S.

REFERENCES

1. **Bhat, K. S., N. K. Bhat, G. R. Kulkarni, A. Iyengar, and N. G. Avadhani.** 1985. Expression of the cytochrome b-URF6-URF5 region of the mouse mitochondrial genome. Biochemistry **24:**5818–5825.
2. **Bollenbach, T. J., G. Schuster, and D. B. Stern.** 2004. Cooperation of endo- and exoribonucleases in chloroplast mRNA turnover. Prog. Nucleic Acid Res. Mol. Biol. **78:**305–337.
3. **Carpousis, A. J., N. F. Vanzo, and L. C. Raynal.** 1999. mRNA degradation, a tale of poly(A) and multiprotein machines. Trends Genet. **15:**24–28.
4. **Cheng, Z. F., and M. P. Deutscher.** 2005. An important role for RNase R in mRNA decay. Mol. Cell **17:**313–318.
5. **Coburn, G. A., and G. A. Mackie.** 1999. Degradation of mRNA in *Escherichia coli*: an old problem with some new twists. Prog. Nucleic Acid Res. **62:**55–108.
6. **Dreyfus, M., and P. Regnier.** 2002. The poly(A) tail of mRNAs: bodyguard in eukaryotes, scavenger in bacteria. Cell **111:**611–613.
7. **Dziembowski, A., J. Piwowarski, R. Hoser, M. Minczuk, A. Dmochowska, M. Siep, H. van der Spek, L. Grivell, and P. P. Stepien.** 2003. The yeast mitochondrial degradosome. Its composition, interplay between RNA helicase and RNase activities and the role in mitochondrial RNA metabolism. J. Biol. Chem. **278:**1603–1611.
8. **Fernandez-Silva, P., J. A. Enriquez, and J. Montoya.** 2003. Replication and transcription of mammalian mitochondrial DNA. Exp. Physiol. **88:**41–56.
9. **Fish, J., N. Raule, and G. Attardi.** 2004. Discovery of a major D-loop replication origin reveals two modes of human mtDNA synthesis. Science **306:**2098–2101.
10. **Gagliardi, D., P. P. Stepien, R. J. Temperley, R. N. Lightowlers, and Z. M. Chrzanowska-Lightowlers.** 2004. Messenger RNA stability in mitochondria: different means to an end. Trends Genet. **20:**260–267.
11. **Guan, M. X., J. A. Enriquez, N. Fischel-Ghodsian, R. S. Puranam, C. P. Lin, M. A. Maw, and G. Attardi.** 1998. The deafness-associated mitochondrial DNA mutation at position 7445, which affects $tRNA^{Ser(UCN)}$ precursor processing, has long-range effects on NADH dehydrogenase subunit ND6 gene expression. Mol. Cell. Biol. **18:**5868–5879.
12. **Helm, M., and G. Attardi.** 2004. Nuclear control of cloverleaf structure of human mitochondrial $tRNA^{(Lys)}$. J. Mol. Biol. **337:**545–560.
13. **Ifergan, I., A. Shafran, G. Jansen, J. H. Hooijberg, G. L. Scheffer, and Y. G. Assaraf.** 2004. Folate deprivation results in the loss of breast cancer resistance protein (BCRP/ABCG2) expression. A role for BCRP in cellular folate homeostasis. J. Biol. Chem. **279:**25527–25534.
14. **Kao, C. Y., and L. K. Read.** 2005. Opposing effects of polyadenylation on the stability of edited and unedited mitochondrial RNAs in *Trypanosoma brucei*. Mol. Cell. Biol. **25:**1634–1644.
15. **Kuhn, J., U. Tengler, and S. Binder.** 2001. Transcript lifetime is balanced between stabilizing stem-loop structures and degradation-promoting polyadenylation in plant mitochondria. Mol. Cell. Biol. **21:**731–742.
16. **Kushner, S. R.** 2002. mRNA decay in *Escherichia coli* comes of age. J. Bacteriol. **184:**4658–4665.
17. **Levinger, L., M. Morl, and C. Florentz.** 2004. Mitochondrial tRNA 3′ end metabolism and human disease. Nucleic Acids Res. **32:**5430–5441.
18. **Lisitsky, I., P. Klaff, and G. Schuster.** 1996. Addition of poly(A)-rich sequences to endonucleolytic cleavage sites in the degradation of spinach chloroplast mRNA. Proc. Natl. Acad. Sci. USA **93:**13398–13403.
19. **Meierhoff, K., S. Felder, T. Nakamura, N. Bechtold, and G. Schuster.** 2003. HCF152, a PPR protein of Arabidopsis involved in processing of chloroplast *psbB-psbT-psbH-petB-petD* RNAs. Plant Cell **15:**1480–1495.
20. **Mohanty, B. K., and S. R. Kushner.** 1999. Analysis of the function of *Escherichia coli* poly(A) polymerase I in RNA metabolism. Mol. Microbiol. **34:**1094–1108.
21. **Mohanty, B. K., and S. R. Kushner.** 2000. Polynucleotide phosphorylase functions both as a 3′ to 5′ exonuclease and a poly(A) polymerase in *Escherichia coli*. Proc. Natl. Acad. Sci. USA **97:**11966–11971.
22. **Mohanty, B. K., V. F. Maples, and S. R. Kushner.** 2004. The Sm-like protein Hfq regulates polyadenylation dependent mRNA decay in *Escherichia coli*. Mol. Microbiol. **54:**905–920.
23. **Montoya, J., G. L. Gaines, and G. Attardi.** 1983. The pattern of transcription of the human mitochondrial rRNA genes reveals two overlapping transcription units. Cell **34:**151–159.
24. **Nagaike, T., T. Suzuki, T. Katoh, and T. Ueda.** 2005. Human mitochondrial mRNAs are stabilized with polyadenylation regulated by mitochondria-specific poly(A) polymerase and polynucleotide phosphorylase. J. Biol. Chem. **280:**19721–19727.
25. **Ojala, D., J. Montoya, and G. Attardi.** 1981. tRNA punctuation model of RNA processing in human mitochondria. Nature **290:**470–474.
26. **Piwowarski, J., P. Grzechnik, A. Dziembowski, A. Dmochowska, M. Minczuk, and P. P. Stepien.** 2003. Human polynucleotide phosphorylase, hPNPase, is localized in mitochondria. J. Mol. Biol. **329:**853–857.
27. **Regnier, P., and C. M. Arraiano.** 2000. Degradation of mRNA in bacteria: emergence of ubiquitous features. Bioessays **22:**235–244.
28. **Rott, R., G. Zipor, V. Portnoy, V. Liveanu, and G. Schuster.** 2003. RNA polyadenylation and degradation in cyanobacteria are similar to the chloroplast but different from *Escherichia coli*. J. Biol. Chem. **278:**15771–15777.
29. **Shadel, G. S., and D. A. Clayton.** 1997. Mitochondrial DNA maintenance in vertebrates. Annu. Rev. Biochem. **66:**409–435.
30. **Sohlberg, B., J. Huang, and S. N. Cohen.** 2003. The *Streptomyces coelicolor* polynucleotide phosphorylase homologue, and not the putative poly(A) polymerase, can polyadenylate RNA. J. Bacteriol. **185:**7273–7278.
31. **Stark, H. J., M. Baur, D. Breitkreutz, N. Mirancea, and N. E. Fusenig.** 1999. Organotypic keratinocyte cocultures in defined medium with regular epidermal morphogenesis and differentiation. J. Investig. Dermatol. **112:**681–691.
32. **Taanman, J. W.** 1999. The mitochondrial genome: structure, transcription, translation and replication. Biochim. Biophys. Acta **1410:**103–123.
33. **Temperley, R. J., S. H. Seneca, K. Tonska, E. Bartnik, L. A. Bindoff, R. N. Lightowlers, and Z. M. Chrzanowska-Lightowlers.** 2003. Investigation of a pathogenic mtDNA microdeletion reveals a translation-dependent deadenylation decay pathway in human mitochondria. Hum. Mol. Genet. **12:**2341–2348.
34. **Tomecki, R., A. Dmochowska, K. Gewartowski, A. Dziembowski, and P. P. Stepien.** 2004. Identification of a novel human nuclear-encoded mitochondrial poly(A) polymerase. Nucleic Acids Res. **32:**6001–6014.
35. **Tullo, A., F. Tanzariello, A. M. D'Erchia, M. Nardelli, P. A. Papeo, E. Sbisa, and C. Saccone.** 1994. Transcription of rat mitochondrial NADH-dehydrogenase subunits. Presence of antisense and precursor RNA species. FEBS Lett. **354:**30–36.
36. **Wickens, M., P. Anderson, and R. J. Jackson.** 1997. Life and death in the cytoplasm: messages from the 3′ end. Curr. Opin. Genet. Dev. **7:**220–232.
37. **Woischnik, M., and C. T. Moraes.** 2002. Pattern of organization of human mitochondrial pseudogenes in the nuclear genome. Genome Res. **12:**885–893.
38. **Yehudai-Resheff, S., M. Hirsh, and G. Schuster.** 2001. Polynucleotide phosphorylase functions as both an exonuclease and a poly(A) polymerase in spinach chloroplasts. Mol. Cell. Biol. **21:**5408–5416.